International Journal of Solids and Structures 47 (2010) 2578–2590

Contents lists available at ScienceDirect

International Journal of Solids and Structures

journal homepage: www.elsevier.com/locate/ijsolstr

The G2 constant displacement discontinuity method – Part II: Solution of half-plane crack problems

G. Exadaktylos *, G. Xiroudakis

Mining Engineering Design Laboratory, Department of Mineral Resources Engineering, Technical University of Crete, GR 73100, Chania, Greece

ARTICLE INFO

Article history:
Available online 24 May 2010

Keywords:
Displacement discontinuity
Strain-gradient elasticity
Crack problems
Stress intensity factors
Half-plane

ABSTRACT

In the previous Part I, the G2 constant displacement discontinuity element was presented that is dedicated for the fast (only one collocation point per element), stable and accurate numerical solution of modes I, II and III cracks of arbitrary shape in an infinite plane isotropic elastic body. Herein, another G2 constant displacement discontinuity element is constructed for the case of cracks in the half-plane. It is successfully validated against existing semi-analytical and numerical solutions of crack problems in the half-plane.

© 2010 Elsevier Ltd. All rights reserved.

1. Introduction

In the previous Part I (Exadaktylos and Xiroudakis, submitted for publication), the G2 constant displacement discontinuity (G2CDD) element was tailored for the analysis of modes I, II and III cracks of arbitrary shape in an infinite plane isotropic elastic body in the context of the displacement discontinuity method (DDM) (Crouch, 1976a,b; Crouch and Starfield, 1990). It is worth mentioning here that DDM belongs to the family of the dual Boundary Element Method (BEM) (Chen and Hong, 1999; Hong and Chen, 1988a,b). The proposed G2 element is based on the strain-gradient elasticity theory, and more specifically on its Grade-2 (G2) variant, and gives considerably more accurate results for the Stress Intensity Factors (SIFs) compared to the classical constant displacement discontinuity (CDD) method. In the following Section 2, the G2CDD approach is further elaborated to incorporate automatically traction-free boundary conditions for a semi-infinite region by using the classical method of images (Hirth and Lothe, 1982; Crouch, 1976a). Finally, in Section 3 it is validated against existing semi-analytical solutions of crack problems in the half-plane. These solutions refer to the pressurized crack parallel to the free surface, the crack normal to the free surface subjected to far-field tension or shear, and the curvilinear crack close to the free surface of the half-plane.

2. The half-plane G2 solution for an arbitrarily inclined finite line segment

For the extension of the G2CDD method to situations in which the region to be analyzed is affected by the proximity of a traction-free plane surface, it is necessary to obtain the solution for a constant displacement discontinuity over an arbitrarily oriented, finite line segment in a semi-infinite body. This solution is constructed by superposition from the infinite body results presented in Part I by using the classical method of images (Hirth and Lothe, 1982). It consists of two parts, namely, the actual solution already found in Part I for an infinite body with a constant displacement discontinuity over an arbitrarily oriented, finite line segment in $y<0$, as is shown in Fig. 1, an "image discontinuity" in $y>0$ that cancels out the shear stresses on $y=0$, and a continuous distribution of normal stress on $y=0$ that cancels out the normal tractions on the free surface of the half plane. Hence, the complete solution is given by the sum of the three separate solutions. The Cauchy stress tensor due to the actual DD will be denoted by $\sigma_{ij(A)}$, while the stress tensor due to its image by $\sigma_{ij(I)}$, and those resulting from the supplemental solution by $\sigma_{ij(S)}$, wherein indices i, j denote the Cartesian coordinates x, y. Then, the complete solution for the half-plane may be represented as follows:

$$\sigma_{ij} = \sigma_{ij(A)} + \sigma_{ij(I)} + \sigma_{ij(S)} \quad i.j = x, y \tag{1}$$

Hereafter, tensile stresses are considered as positive quantities and the unit length is chosen to be the half-width of the DD element, since the sizes of the elements are taken to be equal.

As is illustrated in Fig. 1, local coordinate systems attached on the actual and image finite linear segments are adopted in the following fashion, respectively,

$$\bar{x}_A = x\cos\beta + (y+h)\sin\beta; \quad \bar{y}_A = -x\sin\beta + (y+h)\cos\beta, \tag{2}$$

and

$$\bar{x}_I = x\cos\beta - (y-h)\sin\beta; \quad \bar{y}_I = x\sin\beta + (y-h)\cos\beta. \tag{3}$$

* Corresponding author. Tel.: +30 28210 37690; fax: +30 28210 37891.
E-mail address: exadakty@mred.tuc.gr (G. Exadaktylos).

0020-7683/$ - see front matter © 2010 Elsevier Ltd. All rights reserved.
doi:10.1016/j.ijsolstr.2010.05.014

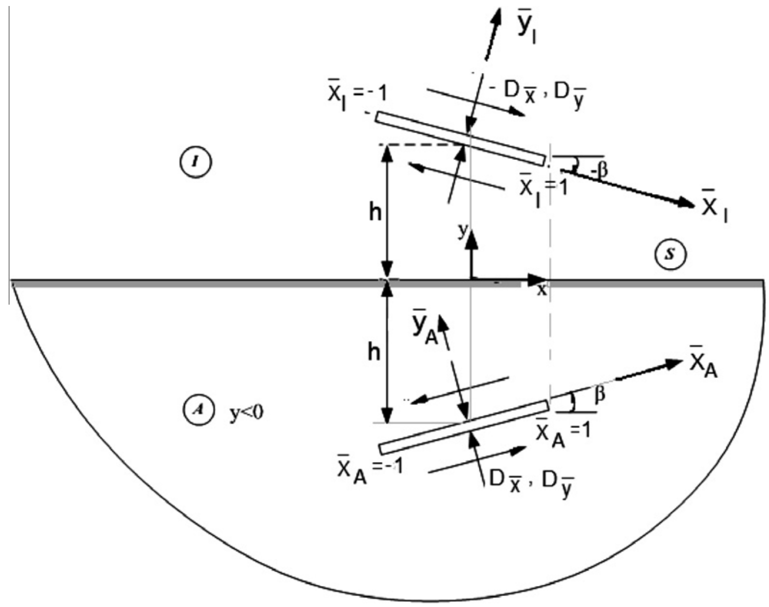

Fig. 1. Arbitrarily oriented finite line segment in the lower half-space with its image in the upper half-plane and coordinate systems.

where β denotes the inclination angle of the straight dislocation w.r.t. the horizontal in the manner shown in Fig. 1 and h is the depth of the dislocation centre. For $y = 0$ the image local coordinates given from Eq. (3), take the following form

$$h_x = x\cos\beta + h\sin\beta; \quad h_y = x\sin\beta - h\cos\beta. \tag{4}$$

The solution for the stresses in plane strain conditions produced by an actual finite straight Mode I dislocation occupying the line segment $-1 < \bar{x}_A < 1,\ \bar{y}_A = 0$ with no loading at infinity and displaying a constant DD of magnitude $D_{\bar{y}}$ may be found from Eq's (2a–c) of Part I (Exadaktylos and Xiroudakis, submitted for publication) by applying the appropriate rotations in order to refer to the global coordinate system Oxy, i.e.

$$\begin{aligned}\sigma^I_{xx(A)}(x,y) = &-\frac{GD_{\bar{y}}}{2(1-\nu)}\sqrt{\frac{2}{\pi}}\int_0^\infty \xi^{1/2}(1+\ell^2\xi^2)(1-\cos(2\beta)|\bar{y}_A|\xi)\\ &\times\cos(\bar{x}_A\xi)J_{1/2}(\xi)e^{-|\bar{y}_A|\xi}d\xi\\ &+\frac{GD_{\bar{y}}}{2(1-\nu)}\sqrt{\frac{2}{\pi}}\int_0^\infty \xi^{3/2}(1+\ell^2\xi^2)\sin(2\beta)\bar{y}_A\\ &\times\sin(\bar{x}_A\xi)J_{1/2}(\xi)e^{-|\bar{y}_A|\xi}d\xi\end{aligned} \tag{5a}$$

$$\begin{aligned}\sigma^I_{xy(A)}(x,y) = &\frac{GD_{\bar{y}}}{2(1-\nu)}\sqrt{\frac{2}{\pi}}|\bar{y}_A|\int_0^\infty \xi^{3/2}(1+\ell^2\xi^2)\\ &\times\sin(2\beta)J_{1/2}(\xi)e^{-|\bar{y}_A|\xi}\cos(\bar{x}_A\xi)d\xi - \frac{GD_{\bar{y}}}{2(1-\nu)}\\ &\times\sqrt{\frac{2}{\pi}}\bar{y}_A\int_0^\infty \xi^{3/2}(1+\ell^2\xi^2)\cos(2\beta)J_{1/2}(\xi)e^{-|\bar{y}_A|\xi}\\ &\times\sin(\bar{x}_A\xi)d\xi\end{aligned} \tag{5b}$$

$$\begin{aligned}\sigma^I_{yy(A)}(x,y) = &-\frac{GD_{\bar{y}}}{2(1-\nu)}\sqrt{\frac{2}{\pi}}\int_0^\infty \xi^{1/2}(1+\ell^2\xi^2)(1+\cos(2\beta)|\bar{y}_A|\xi)\\ &\times\cos(\bar{x}_A\xi)J_{1/2}(\xi)e^{-|\bar{y}_A|\xi}d\xi - \frac{GD_{\bar{y}}}{2(1-\nu)}\sqrt{\frac{2}{\pi}}\\ &\times\int_0^\infty \xi^{3/2}(1+\ell^2\xi^2)\sin(2\beta)\bar{y}_A\sin(\bar{x}_A\xi)J_{1/2}(\xi)e^{-|\bar{y}_A|\xi}d\xi\end{aligned} \tag{5c}$$

Similarly, the solution for image element (Fig. 1) referred to the global coordinate system may be found by substituting the global coordinates in Eq. (2) of Part I (Exadaktylos and Xiroudakis, submitted for publication) with the local coordinates of the image element and applying the appropriate rotation as follows:

$$\begin{aligned}\sigma^I_{xx(I)}(x,y) = &-\frac{GD_{\bar{y}}}{2(1-\nu)}\sqrt{\frac{2}{\pi}}\int_0^\infty \xi^{1/2}(1+\ell^2\xi^2)(1-\cos(2\beta)|\bar{y}_I|\xi)\\ &\times\cos(\bar{x}_I\xi)J_{1/2}(\xi)e^{-|\bar{y}_I|\xi}d\xi\\ &-\frac{GD_{\bar{y}}}{2(1-\nu)}\sqrt{\frac{2}{\pi}}\int_0^\infty \xi^{3/2}(1+\ell^2\xi^2)\sin(2\beta)\bar{y}_I\\ &\times\sin(\bar{x}_I\xi)J_{1/2}(\xi)e^{-|\bar{y}_I|\xi}d\xi\end{aligned} \tag{6a}$$

$$\begin{aligned}\sigma^I_{xy(I)}(x,y) = &-\frac{GD_{\bar{y}}}{2(1-\nu)}\sqrt{\frac{2}{\pi}}|\bar{y}_I|\int_0^\infty \xi^{3/2}(1+\ell^2\xi^2)\\ &\times\sin(2\beta)J_{1/2}(\xi)e^{-|\bar{y}_I|\xi}\cos(\bar{x}_I\xi)d\xi - \frac{GD_{\bar{y}}}{2(1-\nu)}\\ &\times\sqrt{\frac{2}{\pi}}\bar{y}_I\int_0^\infty \xi^{3/2}(1+\ell^2\xi^2)\cos(2\beta)J_{1/2}(\xi)e^{-|\bar{y}_I|\xi}\\ &\times\sin(\bar{x}_I\xi)d\xi\end{aligned} \tag{6b}$$

$$\begin{aligned}\sigma^I_{yy(I)}(x,y) = &-\frac{GD_{\bar{y}}}{2(1-\nu)}\sqrt{\frac{2}{\pi}}\int_0^\infty \xi^{1/2}(1+\ell^2\xi^2)(1+\cos(2\beta)|\bar{y}_I|\xi)\\ &\times\cos(\bar{x}_I\xi)J_{1/2}(\xi)e^{-|\bar{y}_I|\xi}d\xi\\ &+\frac{GD_{\bar{y}}}{2(1-\nu)}\sqrt{\frac{2}{\pi}}\int_0^\infty \xi^{3/2}(1+\ell^2\xi^2)\sin(2\beta)\bar{y}_I\\ &\times\sin(\bar{x}_I\xi)J_{1/2}(\xi)e^{-|\bar{y}_I|\xi}d\xi\end{aligned} \tag{6c}$$

wherein as in Part I the Latin superscript "I" designates a mode I dislocation, G, ν denote the shear modulus and Poisson's ratio of the material, respectively, ℓ is the strain-gradient coefficient that has dimensions of length, ξ is the real-valued transform parameter, and $J_n(\cdot)$ is the usual Bessel function of the first kind and of order n.

It may be easily verified by adding respectively, Eqs. (5b) and (6b) as well as Eqs. (5c) and (6c) that the line $y = 0$ is free from shear tractions and display non-zero normal tractions, since normal stresses produced by the actual and image discontinuities are equal along the line $y = 0$, i.e.

$$
\begin{aligned}
&(\sigma^I_{xy(A)} + \sigma^I_{xy(I)})_{y=0} = 0, \\
&(\sigma^I_{yy(A)} + \sigma^I_{yy(I)})_{y=0} = (2\sigma^I_{yy(A)})_{y=0} = (2\sigma^I_{yy(I)})_{y=0}
\end{aligned} \tag{7}
$$

The above normal tractions may be removed from the line $y = 0$ by superimposing a supplemental (or fictitious) solution for the half-plane $y \geqslant 0$ that has appropriate stress boundary values on $y = 0$. So, we seek the solution of the following stress boundary value problem for the half-plane $y \leqslant 0$

$$
\left.\begin{aligned}
\sigma^I_{xy(S)} &= 0, \\
\sigma^I_{yy(S)} &= -2\sigma^I_{yy(I)}
\end{aligned}\right\} \quad -\infty < x < \infty, \quad y = 0 \tag{8}
$$

The solution of this boundary value problem may be found in Part I (Exadaktylos and Xiroudakis, submitted for publication), to be

$$
\bar{\sigma}^I_{yy(S)}(\xi, y) = -2(1 + |y|\xi)B_2(\xi)e^{|y|\xi} \tag{9}
$$

where the 'bar notation' denotes the one dimensional Fourier transform of stress w.r.t. x coordinate. First, by substituting $y = 0$, and furthermore changing the nature of the gradient length scale by setting $\ell = I|\ell|$ where $|\ell|$ denotes the modulus of the imaginary parameter ℓ, as is explained in (Exadaktylos and Xiroudakis, 2010a), into Eq. (6c) it is derived

$$
\begin{aligned}
\sigma^I_{yy(I)}(x,0) = \frac{GD_{\bar{y}}}{2\pi(1-v)} \Bigg[& \left(\frac{h_x - 1 - h_y\sin(2\beta)}{(h_x-1)^2 + h_y^2} - \frac{h_x + 1 - h_y\sin(2\beta)}{(h_x+1)^2 + h_y^2} \right) \\
& - 2h_y^2 \left(\frac{(h_x-1)\cos(2\beta) + h_y\sin(2\beta)}{((h_x-1)^2 + h_y^2)^2} - \frac{(h_x+1)\cos(2\beta) + h_y\sin(2\beta)}{((h_x+1)^2 + h_y^2)^2} \right) \\
& + 2\ell^2 \Bigg\{ \left(\frac{h_x - 1 - 3h_y\sin(2\beta)}{((h_x-1)^2 + h_y^2)^2} - \frac{h_x + 1 - 3h_y\sin(2\beta)}{((h_x+1)^2 + h_y^2)^2} \right) \\
& - 4h_y^2 \left(\frac{(h_x-1)(1 - 3\cos(2\beta)) + 6h_y\sin(2\beta)}{((h_x-1)^2 + h_y^2)^3} \right. \\
& \left. - \frac{(h_x+1)(1 - 3\cos(2\beta)) + 6h_y\sin(2\beta)}{((h_x+1)^2 + h_y^2)^3} \right) \\
& - 24h_y^4 \left(\frac{(h_x-1)\cos(2\beta) - h_y\sin(2\beta)}{((h_x-1)^2 + h_y^2)^4} - \frac{(h_x+1)\cos(2\beta) - h_y\sin(2\beta)}{((h_x+1)^2 + h_y^2)^4} \right) \Bigg\} \Bigg]
\end{aligned} \tag{10}
$$

where $I \equiv \sqrt{-1}$ is the usual imaginary unit and it was set $|\ell| = \ell$. Then, the only unknown $B_2(\xi)$ is found by requiring $\sigma^I_{yy(S)}(x,0) = -2\sigma^I_{yy(I)}(x,0)$, that is to say

$$
\begin{aligned}
&\sigma^I_{yy(S)}(x,0) = -2\sqrt{\frac{2}{\pi}}\int_0^\infty B_2(\xi)e^{(Ix\xi)}d\xi = -2\sigma^I_{yy(I)}(x,0) \Rightarrow \\
&B_2(\xi) = \sqrt{\frac{2}{\pi}}\int_0^\infty \sigma^I_{yy(I)}(x,0)e^{(-I\xi x)}dx
\end{aligned} \tag{11}
$$

Hence, the function $B_2(\xi)$ for the mode I case could be found analytically in a formal way by substituting in the r.h.s. of Eq. (11) the representation for $\sigma^I_{yy(I)}(x,0)$ given by Eq. (10) and by assuming that $h \geqslant |\sin(\beta)|$ and $\xi > 0$, as follows

$$
\begin{aligned}
B_2(\xi) = & -\sqrt{\frac{2}{\pi}}\frac{GD_{\bar{y}}}{2(1-v)}e^{(-\xi h)}[\sin(e^{(I\beta)}\xi)\cos(\beta) \\
& - Ie^{(-2I\beta)}(\cos(e^{(I\beta)}\xi)\sin(\beta) + I\sin(e^{(I\beta)}\xi)h)e^{(3I\beta)}\xi \\
& + \ell^2\xi^2\{Ie^{(-2I\beta)}(\cos(e^{(I\beta)}\xi)\sin(\beta) + I\sin(e^{(I\beta)}\xi)h) \\
& \times (2\cos(4\beta)e^{(I\beta)} - e^{(-3I\beta)})\xi - \sin(e^{(I\beta)}\xi)(\cos(3\beta) \\
& + 3\sin(2\beta)\sin\beta + 2I\sin(\beta)^3)\}]
\end{aligned} \tag{12}
$$

Finally, the supplementary solution for the stresses for the lower half-plane ($y \leqslant 0$) may be found to be

$$
\begin{aligned}
\sigma^I_{xx(S)}(x,y) &= -2\sqrt{\frac{2}{\pi}}\Re\left\{\int_0^\infty (1 + y\xi)B_2(\xi)\exp(Ix\xi)e^{y\xi}d\xi\right\} \\
\sigma^I_{xy(S)}(x,y) &= -2\Im\left\{\sqrt{\frac{2}{\pi}}\int_0^\infty (y\xi)B_2(\xi)\exp(Ix\xi)e^{y\xi}d\xi\right\} \\
\sigma^I_{yy(S)}(x,y) &= -2\Re\left\{\sqrt{\frac{2}{\pi}}\int_0^\infty (1 - y\xi)B_2(\xi)\exp(Ix\xi)e^{y\xi}d\xi\right\}
\end{aligned} \tag{13}
$$

in which $\Re$, $\Im$ denote the real and imaginary values of what they enclose, respectively. The analytical solutions of above semi-infinite integrals may be found as follows:

$$
\begin{aligned}
\sigma^I_{xx(S)}(x,y) = & -\frac{GD_{\bar{y}}}{2\pi(1-v)}\Re\Bigg\{\Bigg(\frac{2\cos(\beta)}{(x - \cos(\beta)) + I(h - y - \sin(\beta))} \\
& - \frac{2\cos(\beta)}{(x + \cos(\beta)) + I(h - y + \sin(\beta))}\Bigg) \\
& + 2I\left(\frac{e^{(I\beta)}(h - \sin(\beta)) + y\cos(\beta)}{((x - \cos(\beta)) + I(h - y - \sin(\beta)))^2}\right. \\
& \left. - \frac{e^{(I\beta)}(h + \sin(\beta)) + y\cos(\beta)}{((x + \cos(\beta)) + I(h - y + \sin(\beta)))^2}\right) \\
& - 4y\left(\frac{e^{I\beta}(h - \sin(\beta))}{((x - \cos(\beta)) + I(h - y - \sin(\beta)))^3}\right. \\
& \left. - \frac{e^{I\beta}(h + \sin(\beta))}{((x + \cos(\beta)) + I(h - y + \sin(\beta)))^3}\right) \\
& + 2\ell^2\Bigg[-\left(\frac{e^{(3I\beta)} - 3e^{(I\beta)}}{((x - \cos(\beta)) + I(h - y - \sin(\beta)))^3}\right. \\
& \left. - \frac{e^{(3I\beta)} - 3e^{(I\beta)}}{((x + \cos(\beta)) + I(h - y + \sin(\beta)))^3}\right) \\
& + 3I\left(\frac{2e^{(3I\beta)}(h - \sin(\beta)) - y(e^{(3I\beta)} - 3e^{(I\beta)})}{((x - \cos(\beta)) + I(h - y - \sin(\beta)))^4}\right. \\
& \left. - \frac{2e^{(3I\beta)}(h + \sin(\beta)) - y(e^{(3I\beta)} - 3e^{(I\beta)})}{((x + \cos(\beta)) + I(h - y + \sin(\beta)))^4}\right) \\
& - 24y\left(\frac{e^{3I\beta}(h - \sin(\beta))}{((x - \cos(\beta)) + I(h - y - \sin(\beta)))^5}\right. \\
& \left. - \frac{e^{3I\beta}(h + \sin(\beta))}{((x + \cos(\beta)) + I(h - y + \sin(\beta)))^5}\right)\Bigg]\Bigg\}
\end{aligned} \tag{14a}
$$

$$
\begin{aligned}
\sigma^I_{xy(S)}(x,y) = & -\frac{GD_{\bar{y}}y}{2\pi(1-v)}\Im\Bigg\{\Bigg(\frac{2I\cos(\beta)}{((x - \cos(\beta)) + I(h - y - \sin(\beta)))^2} \\
& - \frac{2I\cos(\beta)}{((x + \cos(\beta)) + I(h - y + \sin(\beta)))^2}\Bigg) \\
& - 4\left(\frac{e^{(I\beta)}(h - \sin(\beta))}{((x - \cos(\beta)) + I(h - y - \sin(\beta)))^3}\right. \\
& \left. - \frac{e^{(I\beta)}(h + \sin(\beta))}{((x + \cos(\beta)) + I(h - y + \sin(\beta)))^3}\right) \\
& + 6\ell^2\Bigg[-I\left(\frac{e^{(3I\beta)} - 3e^{(I\beta)}}{((x - \cos(\beta)) + I(h - y - \sin(\beta)))^4}\right. \\
& \left. - \frac{e^{(3I\beta)} - 3e^{(I\beta)}}{((x + \cos(\beta)) + I(h - y + \sin(\beta)))^4}\right) \\
& - 8\left(\frac{e^{3I\beta}(h - \sin(\beta))}{((x - \cos(\beta)) + I(h - y - \sin(\beta)))^5}\right. \\
& \left. - \frac{e^{3I\beta}(h + \sin(\beta))}{((x + \cos(\beta)) + I(h - y + \sin(\beta)))^5}\right)\Bigg]\Bigg\}
\end{aligned} \tag{14b}
$$

$$
\begin{aligned}
\sigma^{I}_{yy(S)}(x,y) = & -\frac{GD_{\bar{y}}}{2\pi(1-\upsilon)}\Re\Bigg\{\Bigg(\frac{2\cos(\beta)}{(x-\cos(\beta))+I(h-y-\sin(\beta))} \\
& -\frac{2\cos(\beta)}{(x+\cos(\beta))+I(h-y+\sin(\beta))}\Bigg) \\
& +2I\Bigg(\frac{e^{(I\beta)}(h-\sin(\beta))-y\cos(\beta)}{((x-\cos(\beta))+I(h-y-\sin(\beta)))^2} \\
& -\frac{e^{(I\beta)}(h+\sin(\beta))-y\cos(\beta)}{((x+\cos(\beta))+I(h-y+\sin(\beta)))^2}\Bigg) \\
& +4y\Bigg(\frac{e^{I\beta}(h-\sin(\beta))}{((x-\cos(\beta))+I(h-y-\sin(\beta)))^3} \\
& -\frac{e^{I\beta}(h+\sin(\beta))}{((x+\cos(\beta))+I(h-y+\sin(\beta)))^3}\Bigg) \\
& +2\ell^2\Bigg[-\Bigg(\frac{e^{(3I\beta)}-3e^{(I\beta)}}{((x-\cos(\beta))+I(h-y-\sin(\beta)))^3} \\
& -\frac{e^{(3I\beta)}-3e^{(I\beta)}}{((x+\cos(\beta))+I(h-y+\sin(\beta)))^3}\Bigg) \\
& +3I\Bigg(\frac{2e^{(3I\beta)}(h-\sin(\beta))+y(e^{(3I\beta)}-3e^{(I\beta)})}{((x-\cos(\beta))+I(h-y-\sin(\beta)))^4} \\
& -\frac{2e^{(3I\beta)}(h+\sin(\beta))+y(e^{(3I\beta)}-3e^{(I\beta)})}{((x+\cos(\beta))+I(h-y+\sin(\beta)))^4}\Bigg) \\
& + \quad 24y\Bigg(\frac{e^{3I\beta}(h-\sin(\beta))}{((x-\cos(\beta))+I(h-y-\sin(\beta)))^5} \\
& -\frac{e^{3I\beta}(h+\sin(\beta))}{((x+\cos(\beta))+I(h-y+\sin(\beta)))^5}\Bigg)\Bigg]\Bigg\} \qquad (14c)
\end{aligned}
$$

For brevity of the presentation, the analytical expressions of the supplemental stresses derived after evaluating in an explicit manner the real and imaginary parts of Eqs. (14) above, are presented in Appendix A.

Proceeding further, the solution referring to the global coordinate system Oxy for the stresses in plane strain conditions, produced by an arbitrarily oriented finite straight Mode II dislocation lying in the lower half-plane and occupying the line segment $-1 < \bar{x}_A < 1,\ \bar{y}_A = 0$ with no loading at infinity and displaying a constant DD of magnitude $D_{\bar{x}}$ in local coordinates (Fig. 1) may be found from Eq's (4a–c) of Part I (Exadaktylos and Xiroudakis, submitted for publication) by applying the appropriate rotations in order to refer to the global coordinate system Oxy, i.e.

$$
\begin{aligned}
\sigma^{II}_{xx(A)}(x,y) = & +\frac{GD_{\bar{x}}}{2(1-\upsilon)}\sqrt{\frac{2}{\pi}}\int_0^\infty \xi^{1/2}(1+l^2\xi^2)J_{1/2}(\xi) \\
& \times(1-\bar{y}_A\xi)\sin(2\beta)\cos(\bar{x}_A\xi)e^{-\bar{y}_A\xi}d\xi \\
& -\frac{GD_{\bar{x}}}{2(1-\upsilon)}\sqrt{\frac{2}{\pi}}\int_0^\infty \xi^{1/2}(1+l^2\xi^2)J_{1/2}(\xi)(2\cos^2\beta-\bar{y}_A\xi \\
& \times\cos(2\beta))\sin(\bar{x}_A\xi)e^{-\bar{y}_A\xi}d\xi\,\sigma^{II}_{xy(A)}(x,y) \\
& = -\frac{GD_{\bar{x}}}{2(1-\upsilon)}\sqrt{\frac{2}{\pi}}\int_0^\infty \xi^{1/2}(1+l^2\xi^2)J_{1/2}(\xi)(1-\bar{y}_A\xi) \\
& \times\cos(2\beta)\cos(\bar{x}_A\xi)e^{-\bar{y}_A\xi}d\xi \\
& -\frac{GD_{\bar{x}}}{2(1-\upsilon)}\sqrt{\frac{2}{\pi}}\int_0^\infty \xi^{1/2}(1+l^2\xi^2)J_{1/2}(\xi)(1-\bar{y}_A\xi) \\
& \times\sin(2\beta)\sin(\bar{x}_A\xi)e^{-\bar{y}_A\xi}d\xi \qquad (15a)
\end{aligned}
$$

$$
\begin{aligned}
\sigma^{II}_{yy(A)}(x,y) = & -\frac{GD_{\bar{x}}}{2(1-\upsilon)}\sqrt{\frac{2}{\pi}}\int_0^\infty \xi^{1/2}(1+l^2\xi^2)J_{1/2}(\xi)(1-\bar{y}_A\xi) \\
& \times\sin 2\beta\cos\bar{x}_A\xi e^{-\bar{y}_A\xi}d\xi+\frac{GD_{\bar{x}}}{2(1-\upsilon)}\sqrt{\frac{2}{\pi}} \\
& \times\int_0^\infty \xi^{1/2}(1+l^2\xi^2)J_{1/2}(\xi)(2\sin^2\beta \\
& +\bar{y}_A\xi\cos 2\beta)\sin\bar{x}_A\xi e^{-\bar{y}_A\xi}d\xi \qquad (15b)
\end{aligned}
$$

Similarly, the solution for image element (Fig. 1) referred also to the global coordinate system, could be found by substituting the global coordinates in Eq. (4) of Part I with the local coordinates of the image element lying in the upper half-plane and applying the appropriate rotation in the following manner:

$$
\begin{aligned}
\sigma^{II}_{xx(I)}(x,y) = & +\frac{GD_{\bar{x}}}{2(1-\upsilon)}\sqrt{\frac{2}{\pi}}\int_0^\infty \xi^{1/2}(1+l^2\xi^2)J_{1/2}(\xi)(1-\bar{y}_I\xi) \\
& \times\sin 2\beta\cos\bar{x}_I\xi e^{-\bar{y}_I\xi}d\xi+\frac{GD_{\bar{x}}}{2(1-\upsilon)}\sqrt{\frac{2}{\pi}} \\
& \times\int_0^\infty \xi^{1/2}(1+l^2\xi^2)J_{1/2}(\xi)(2\cos^2\beta-\bar{y}_I\xi\cos 2\beta) \\
& \times\sin\bar{x}_I\xi e^{-\bar{y}_I\xi}d\xi \qquad (16a)
\end{aligned}
$$

$$
\begin{aligned}
\sigma^{II}_{xy(I)}(x,y) = & +\frac{GD_{\bar{x}}}{2(1-\upsilon)}\sqrt{\frac{2}{\pi}}\int_0^\infty \xi^{1/2}(1+l^2\xi^2)J_{1/2}(\xi) \\
& \times(1-\bar{y}_I\xi)\cos(2\beta)\cos(\bar{x}_I\xi)e^{-\bar{y}_I\xi}d\xi \\
& -\frac{GD_{\bar{x}}}{2(1-\upsilon)}\sqrt{\frac{2}{\pi}}\int_0^\infty \xi^{1/2}(1+l^2\xi^2)J_{1/2}(\xi)(1-\bar{y}_I\xi) \\
& \times\sin(2\beta)\sin(\bar{x}_I\xi)e^{-\bar{y}_I\xi}d\xi \qquad (16b)
\end{aligned}
$$

$$
\begin{aligned}
\sigma^{II}_{yy(I)}(x,y) = & -\frac{GD_{\bar{x}}}{2(1-\upsilon)}\sqrt{\frac{2}{\pi}}\int_0^\infty \xi^{1/2}(1+l^2\xi^2)J_{1/2}(\xi)(1-\bar{y}_I\xi) \\
& \times\sin(2\beta)\cos(\bar{x}_I\xi)e^{-\bar{y}_I\xi}d\xi+\frac{GD_{\bar{x}}}{2(1-\upsilon)}\sqrt{\frac{2}{\pi}} \\
& \times\int_0^\infty \xi^{1/2}(1+l^2\xi^2)J_{1/2}(\xi)(2\sin^2\beta+\bar{y}_I\xi\cos(2\beta)) \\
& \times\sin(\bar{x}^I\xi)e^{-\bar{y}_I\xi}d\xi \qquad (16c)
\end{aligned}
$$

As in the mode I case, the total shear stress vanishes along the free surface $y = 0$, but the total normal stress still does not vanish at the free surface, that is to say Eq. (7) hold also true for the mode II case. The normal stress may be removed from the line $y = 0$ by superimposing a supplemental (or fictitious) solution for the half-plane $y \geqslant 0$ that has appropriate stress boundary values on $y = 0$. For this purpose, we seek the solution of the following stress boundary value problem for the half-plane $y \leqslant 0$

$$
\left.\begin{aligned}
\sigma^{II}_{xy(S)} &= 0, \\
\sigma^{II}_{yy(S)} &= -2\sigma^{II}_{yy(I)}
\end{aligned}\right\} \quad -\infty < x < \infty, \quad y = 0 \qquad (17)
$$

The solution of this boundary value problem may be also found in Part I (Exadaktylos and Xiroudakis, submitted for publication), that is

$$
\bar{\sigma}^{II}_{yy(S)}(x,y) = 2I(1+|y|\xi)B_1(\xi)e^{|y|\xi} \qquad (18)
$$

For this purpose, first the values $y = 0$ and $\ell = I|\ell|$, where $|\ell|$ denotes the modulus of the imaginary parameter ℓ as in the mode I dislocation, are substituted in Eq. (16c), and the result is evaluated analytically in the following manner,

$$
\begin{aligned}
\sigma^{II}_{yy(I)}(x,y) = & -\frac{GD_{\bar{x}}}{2\pi(1-\nu)}\left[\left(\frac{(1-2cos(2\beta))h_y + sin(2\beta)(h_x+1)}{h_y^2+(h_x+1)^2}\right.\right.\\
& -\left.\frac{(1-2cos(2\beta))h_y + sin(2\beta)(h_x-1)}{h_y^2+(h_x-1)^2}\right)\\
& +2h_y^2\left(\frac{cos(2\beta)h_y - sin(2\beta)(h_x+1)}{(h_y^2+(h_x+1)^2)^2}\right.\\
& -\left.\frac{cos(2\beta)h_y - sin(2\beta)(h_x-1)}{(h_y^2+(h_x-1)^2)^2}\right)\\
& +2\ell^2\left\{\left(\frac{(1-2cos(2\beta))h_y + sin(2\beta)(h_x+1)}{(h_y^2+(h_x+1)^2)^2}\right.\right.\\
& -\left.\frac{(1-2cos(2\beta))h_y + sin(2\beta)(h_x-1)}{(h_y^2+(h_x-1)^2)^2}\right)\\
& -4h_y^2\left(\frac{(1-7cos(2\beta))h_y + 4sin(2\beta)(h_x+1)}{(h_y^2+(h_x+1)^2)^3}\right.\\
& -\left.\frac{(1-7cos(2\beta))h_y + 4sin(2\beta)(h_x-1)}{(h_y^2+(h_x-1)^2)^3}\right)\\
& -24h_y^4\left(\frac{cos(2\beta)h_y - sin(2\beta)(h_x+1)}{(h_y^2+(h_x+1)^2)^4}\right.\\
& -\left.\left.\left.\frac{cos(2\beta)h_y - sin(2\beta)(h_x-1)}{(h_y^2+(h_x-1)^2)^4}\right)\right\}\right]
\end{aligned}
\tag{19}
$$

wherein it was set $|\ell| = \ell$.

Next, the r.h.p. of the above equation is substituted into the second of Eqs. (17) and the resulting equation is solved w.r.t. $B_1(\xi)$ after applying the inverse Fourier transform,

$$
\begin{aligned}
\sigma^{II}_{yy(S)}(x,0) &= 2I\sqrt{\frac{2}{\pi}}\int_0^\infty B_1(\xi)e^{(Ix\xi)}d\xi = -2\sigma^{II}_{yy(I)}(x,0) \Rightarrow B_1(\xi)\\
&= I\sqrt{\frac{2}{\pi}}\int_0^\infty \sigma^{II}_{yy(I)}(x,0)e^{(-I\xi x)}dx
\end{aligned}
\tag{20}
$$

Hence, the function B_1 for mode II case may be found by assuming that $h \geqslant |\sin(\beta)|$ and $\xi > 0$ in the following fashion

$$
\begin{aligned}
B_1(\xi) = & -I\sqrt{\frac{2}{\pi}}\frac{GD_{\bar{x}}}{2(1-\nu)}e^{(-\xi h)}[-(cos(e^{(I\beta)}\xi)sin(\beta)\\
& + Isin(e^{(I\beta)}\xi)h)e^{(-2I\beta)}e^{(3I\beta)}\xi. + sin(e^{(I\beta)}\xi)sin(\beta)\\
& + \ell^2\xi^2\{Ie^{(-2I\beta)}(2e^{(I\beta)}cos(4\beta) - e^{(-3I\beta)})(sin(\xi e^{(I\beta)})h\\
& - Isin(\beta)cos(\xi e^{(I\beta)}))\xi. + sin(\xi e^{(I\beta)})sin(\beta)e^{(2I\beta)}\}]
\end{aligned}
\tag{21}
$$

Subsequently, the supplemental stress solution can be easily found as follows:

$$
\begin{aligned}
\sigma^{II}_{xx(S)}(x,y) &= -2\sqrt{\frac{2}{\pi}}\Im\left\{\int_0^\infty (1+y\xi)B_1(\xi)\exp(Ix\xi)e^{y\xi}d\xi\right\}\\
\sigma^{II}_{xy(S)}(x,y) &= 2\Re\left\{\sqrt{\frac{2}{\pi}}\int_0^\infty (y\xi)B_1(\xi)\exp(Ix\xi)e^{y\xi}d\xi\right\}\\
\sigma^{II}_{yy(S)}(x,y) &= -2\Im\left\{\sqrt{\frac{2}{\pi}}\int_0^\infty (1-y\xi)B_1(\xi)\exp(Ix\xi)e^{y\xi}d\xi\right\}
\end{aligned}
\tag{22}
$$

The analytical forms of the above semi-infinite integrals are the following

$$
\begin{aligned}
\sigma^{II}_{xx(S)}(x,y) = & -\frac{GD_{\bar{x}}}{2\pi(1-\nu)}\Im\left\{\left(\frac{2Isin(\beta)}{(x-\cos(\beta))+I(h-y-\sin(\beta))}\right.\right.\\
& -\left.\frac{2Isin(\beta)}{(x+\cos(\beta))+I(h-y+\sin(\beta))}\right)\\
& +2I\left(\frac{(e^{(I\beta)}(h-sin(\beta))+Iysin(\beta))}{((x-\cos(\beta))+I(h-y-\sin(\beta)))^2}\right.\\
& -\left.\frac{(e^{(I\beta)}(h+sin(\beta))+Iysin(\beta))}{((x+\cos(\beta))+I(h-y+\sin(\beta)))^2}\right)\\
& -4y\left(\frac{(h-sin(\beta))e^{(I\beta)}}{((x-\cos(\beta))+I(h-y-\sin(\beta)))^3}\right.\\
& -\left.\frac{(h+sin(\beta))e^{(I\beta)}}{((x+\cos(\beta))+I(h-y+\sin(\beta)))^3}\right)\\
& +4\ell^2\left[-I\left(\frac{sin(\beta)e^{(2I\beta)}}{((x-\cos(\beta))+I(h-y-\sin(\beta)))^3}\right.\right.\\
& -\left.\frac{sin(\beta)e^{(2I\beta)}}{((x+\cos(\beta))+I(h-y+\sin(\beta)))^3}\right)\\
& +3I\left(\frac{e^{(3I\beta)}(h-sin(\beta))-Iysin(\beta)e^{(2I\beta)}}{((x-\cos(\beta))+I(h-y-\sin(\beta)))^4}\right.\\
& -\left.\frac{e^{(3I\beta)}(h+sin(\beta))-Iysin(\beta)e^{(2I\beta)}}{((x+\cos(\beta))+I(h-y+\sin(\beta)))^4}\right)\\
& -12y\left(\frac{e^{(3I\beta)}(h-sin(\beta))}{((x-\cos(\beta))+I(h-y-\sin(\beta)))^5}\right.\\
& -\left.\left.\left.\frac{e^{(3I\beta)}(h+sin(\beta))}{((x+\cos(\beta))+I(h-y+\sin(\beta)))^5}\right)\right]\right\}
\end{aligned}
\tag{23a}
$$

$$
\begin{aligned}
\sigma^{II}_{xy(S)}(x,y) = & -\frac{GD_{\bar{x}}y}{2\pi(1-\nu)}\Re\left\{2\left(\frac{sin(\beta)}{((x-\cos(\beta))+I(h-y-\sin(\beta)))^2}\right.\right.\\
& -\left.\frac{sin(\beta)}{((x+\cos(\beta))+I(h-y+\sin(\beta)))^2}\right)\\
& +4\left(\frac{(h-sin(\beta))e^{(I\beta)}}{((x-\cos(\beta))+I(h-y-\sin(\beta)))^3}\right.\\
& -\left.\frac{(h+sin(\beta))e^{(I\beta)}}{((x+\cos(\beta))+I(h-y+\sin(\beta)))^3}\right)12\ell^2\\
& \times\left[-\left(\frac{sin(\beta)e^{(2I\beta)}}{((x-\cos(\beta))+I(h-y-\sin(\beta)))^4}\right.\right.\\
& -\left.\frac{sin(\beta)e^{(2I\beta)}}{((x+\cos(\beta))+I(h-y+\sin(\beta)))^4}\right)\\
& +4\left(\frac{(h-sin(\beta))e^{(3I\beta)}}{((x-\cos(\beta))+I(h-y-\sin(\beta)))^5}\right.\\
& -\left.\left.\left.\frac{(h+sin(\beta))e^{(3I\beta)}}{((x+\cos(\beta))+I(h-y+\sin(\beta)))^5}\right)\right]\right\}
\end{aligned}
\tag{23b}
$$

$$
\begin{aligned}
\sigma^{II}_{yy(S)}(x,y) = &-\frac{GD_{\bar{x}}}{2\pi(1-\nu)}\Im\Bigg\{\left(\frac{2I\sin(\beta)}{(x-\cos(\beta))+I(h-y-\sin(\beta))}-\frac{2I\sin(\beta)}{(x+\cos(\beta))+I(h-y+\sin(\beta))}\right)\\
&+2\left(\frac{(y\sin(\beta)+Ie^{(I\beta)}(h-\sin(\beta)))}{((x-\cos(\beta))+I(h-y-\sin(\beta)))^2}-\frac{(y\sin(\beta)+Ie^{(I\beta)}(h+\sin(\beta)))}{((x+\cos(\beta))+I(h-y+\sin(\beta)))^2}\right)\\
&+4y\left(\frac{(h-\sin(\beta))e^{(I\beta)}}{((x-\cos(\beta))+I(h-y-\sin(\beta)))^3}-\frac{(h+\sin(\beta))e^{(I\beta)}}{((x+\cos(\beta))+I(h-y+\sin(\beta)))^3}\right)\\
&+4\ell^2\Bigg[-\left(\frac{I\sin(\beta)e^{(2I\beta)}}{((x-\cos(\beta))+I(h-y-\sin(\beta)))^3}-\frac{I\sin(\beta)e^{(2I\beta)}}{((x+\cos(\beta))+I(h-y+\sin(\beta)))^3}\right)\\
&-3\left(\frac{y\sin(\beta)e^{(2I\beta)}-I(h-\sin(\beta))e^{(3I\beta)}}{((x-\cos(\beta))+I(h-y-\sin(\beta)))^4}-\frac{y\sin(\beta)e^{(2I\beta)}-I(h+\sin(\beta))e^{(3I\beta)}}{((x+\cos(\beta))+I(h-y+\sin(\beta)))^4}\right)\\
&+12y\left(\frac{e^{(3I\beta)}(h-\sin(\beta))}{((x-\cos(\beta))+I(h-y-\sin(\beta)))^5}-\frac{e^{(3I\beta)}(h+\sin(\beta))}{((x+\cos(\beta))+I(h-y+\sin(\beta)))^5}\right)\Bigg]\Bigg\} \qquad (23c)
\end{aligned}
$$

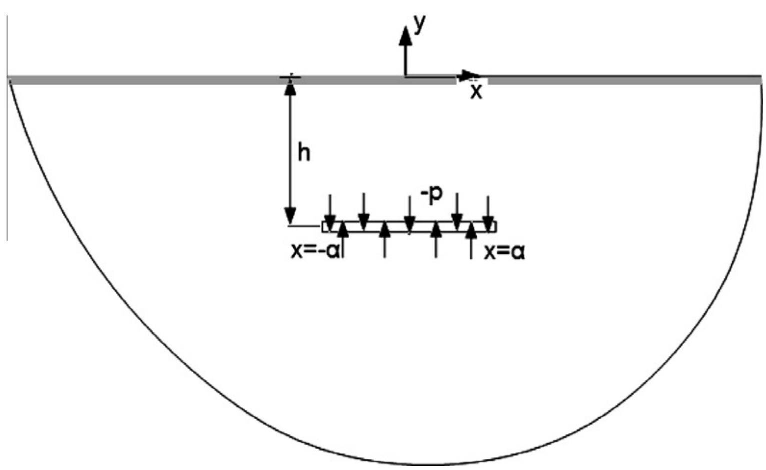

Fig. 2. Geometry and coordinate system for the uniformly pressurized horizontal crack parallel to the free surface and lying in the lower half-plane.

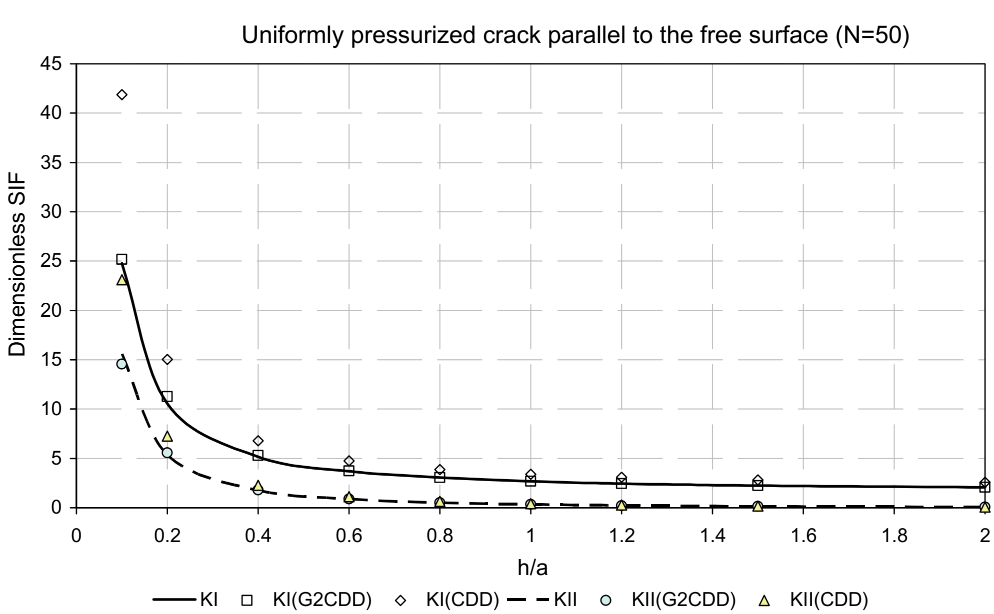

Fig. 3. Dependence of mode I and II SIF's on the dimensionless distance of the crack from the free surface as is computed with classical and special gradient elasticity elements with $N = 50$ elements.

As in the mode I case, the analytical expressions of the above supplemental stresses after the evaluation of their real and imaginary parts, are presented in Appendix A.

3. Validation of the G2CDD method against solutions of half-plane crack problems

Problems pertaining to a half-plane with cracks – even intersecting cracks – subjected to complex loading conditions, are solved almost trivially by the DD method. Each crack is divided into a series of segments in the form of dislocations over which stress boundary conditions are known, and Eq. (13) in Part I (Exadaktylos and Xiroudakis, submitted for publication) with influence coefficients appropriately modified according to the formulae presented in the previous Section, are solved for the discontinuity components at each segment. Stresses elsewhere in the body then can be computed by equations analogous to Eq. (12) of Part I (Exadaktylos and Xiroudakis, submitted for publication) by summing the contributions of all the individual discontinuities. The equations derived here were also implemented into G2TWODD computer code that is dedicated for fast calculations of SIF's and stresses of cracked elastic bodies. In this section, three indicative numerical examples are presented to illustrate the improved accuracy referring to the determination of SIFs with the G2CDD method when compared with the CDD method.

3.1. Straight crack parallel to the free surface

The first problem that is used as a validation example of the proposed numerical method, is the straight crack which is parallel to the stress-free boundary of the half-plane and is subjected to uniform internal pressure $-p(p > 0)$ as is displayed in Fig. 2. This problem is relevant to the fundamental rock mechanical problem of cracks or joints pressurized by the fluid that may contain (e.g.

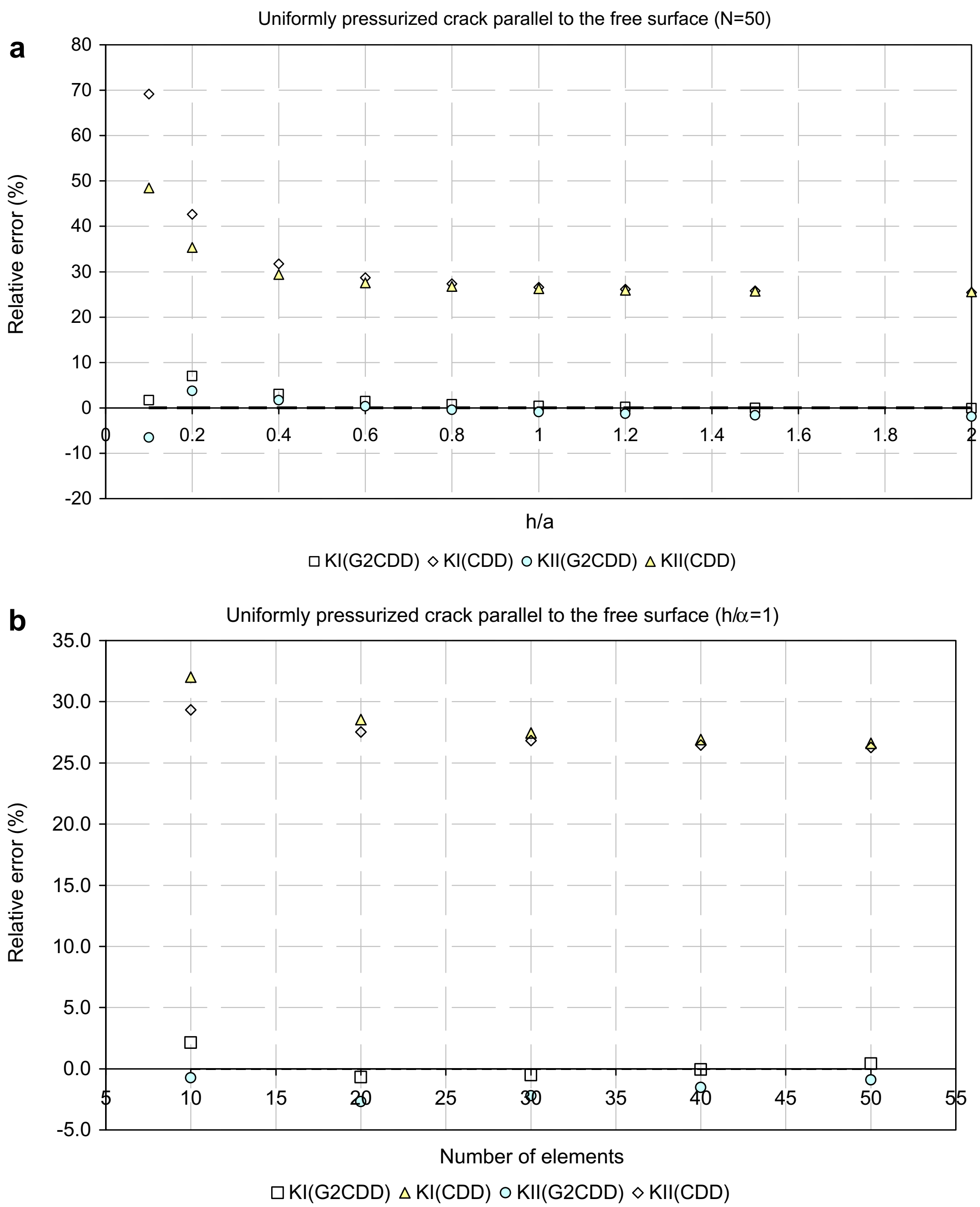

Fig. 4. Variation of the relative error of modes I and II SIFs for horizontal crack with (a) relative crack depth for $N = 50$, and (b) number of discretization elements with $h/\alpha = 1$.

water) and lying near the free-surface of the wall of an excavation or borehole.

Fig. 3 presents the variation of the dimensionless mode I and II SIFs $(K_i/(p\sqrt{a}), i = I, II)$ on the relative crack distance (h/α) from the stress-free surface ($y = 0$) as they are predicted by the G2CDD, and CDD methods, while the crack was discretized by 50 mode I dislocation elements. The continuous and dashed curves present the semi-analytical solution referring to the mode I and II SIF's, respectively, proposed by Itou (1994). This author solved quite accurately this specific problem by using the Fourier transform technique and the theory of dual integral eqns. It is worth noticing that for low values of h/α, the presence a mode II SIF is quite appreciable, while it attenuates fast as $h/\alpha > 0.5$. The very good agreement of the G2CDD results with the semi-analytical solutions may be seen from this figure, as well as from Fig. 4a and b in which the relative error (relative error = (computed value–analytical value)/analytical value x 100) is plotted w.r.t. h/α for $N = 50$ and w.r.t. the number of discretization elements, N, for fixed relative distance equal to 0.1, respectively.

3.2. Straight crack normal to the free surface

The second half-plane problem that is considered here is illustrated in Fig. 5. This case refers to the straight crack normal to the free-surface of the half-plane subjected to uniform horizontal tension and in-plane shear stress at infinity. The closed form expressions for the mode I, and II SIFs at crack tips A and B are given as follows, respectively

$$\begin{Bmatrix} K_I \\ K_{II} \end{Bmatrix}_A = \begin{Bmatrix} \sigma \\ \tau \end{Bmatrix} \sqrt{\pi\alpha} \begin{Bmatrix} F_A(h/a) \\ F_A(h/a) \end{Bmatrix}$$
$$\begin{Bmatrix} K_I \\ K_{II} \end{Bmatrix}_B = \begin{Bmatrix} \sigma \\ \tau \end{Bmatrix} \sqrt{\pi\alpha} \begin{Bmatrix} F_B(h/a) \\ F_B(h/a) \end{Bmatrix} \quad (24)$$

wherein α, h stand for the half-length of the crack and its depth from the free surface, respectively, σ denotes the far-field horizontal tension, τ the far-field in-plane shear stress, whereas the configuration correction factors referring to the tips A, B are denoted as $F_A(h/\alpha)$, $F_B(h/\alpha)$, respectively and are given by Tada et al. (1973). It is

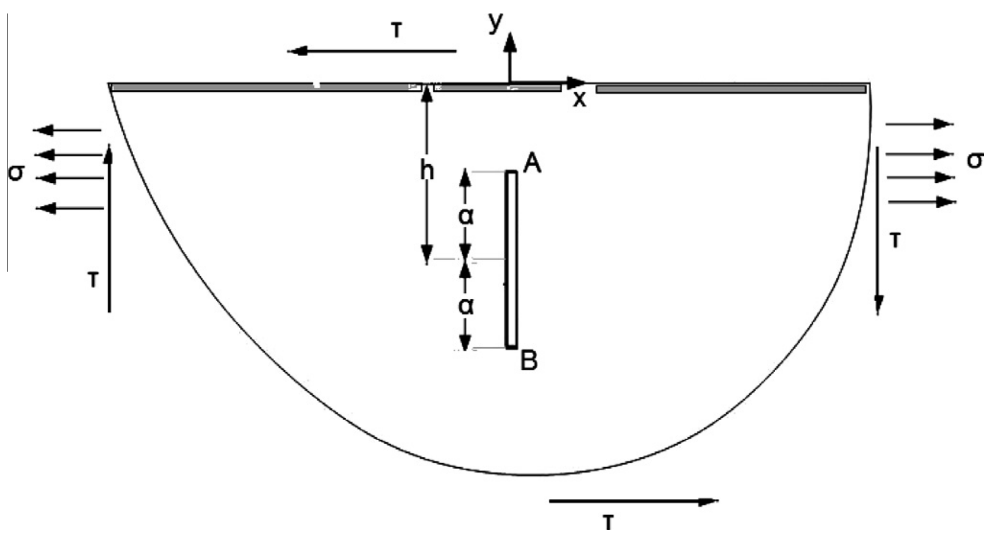

Fig. 5. Straight crack of length 2α normal to the free surface of the half-plane subjected to far-field uniform horizontal tension σ and in-plane shear stress τ.

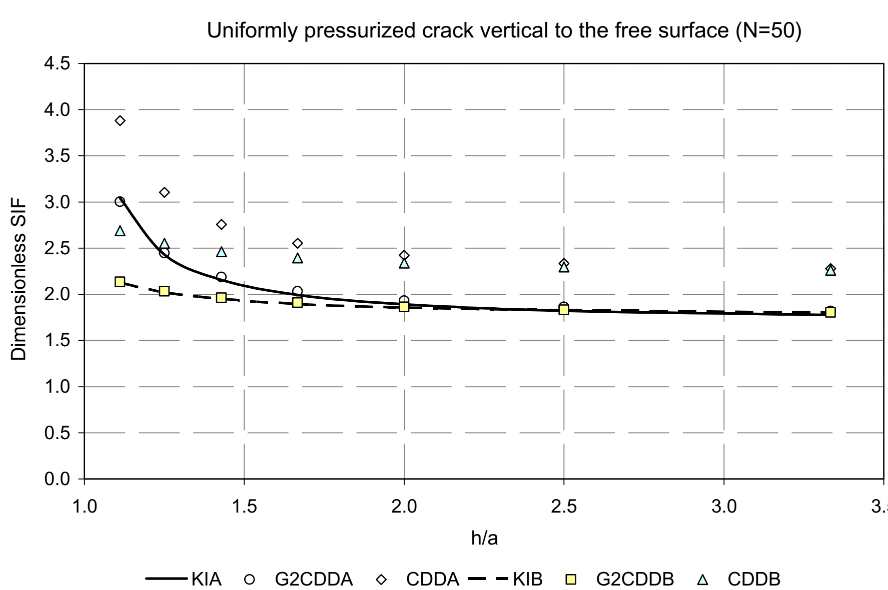

Fig. 6. Comparison of the dependence of mode I SIF at the two tips A, B of the vertical crack discretized with $N = 50$ elements, on its relative distance from the free surface predicted by the semi-analytical solution (continuous and dashed lines) and the two numerical methods CDD and G2CDD.

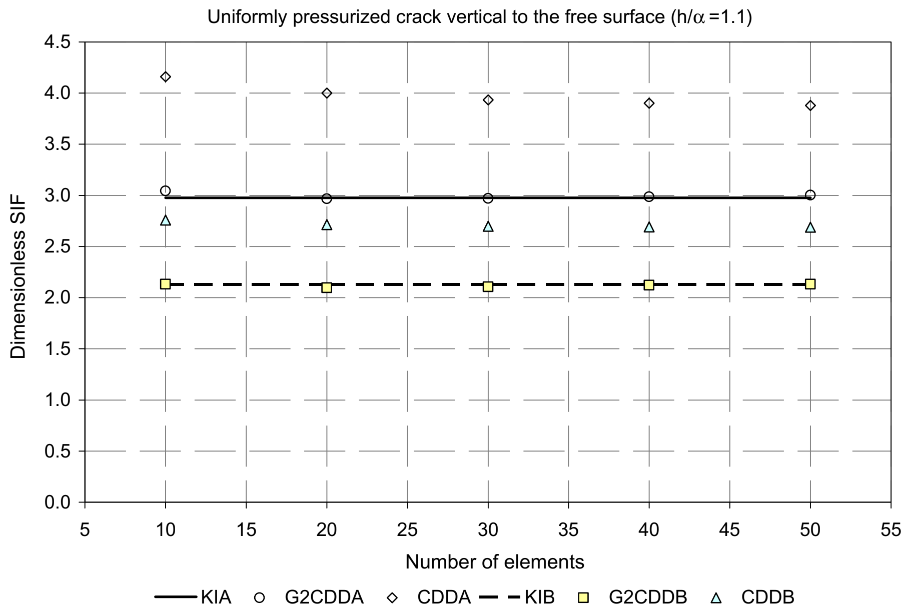

Fig. 7. Dependence of the mode I SIF at the two crack tips A, B on the number of discretization elements for a fixed dimensionless depth of the crack $h/\alpha = 1.1$.

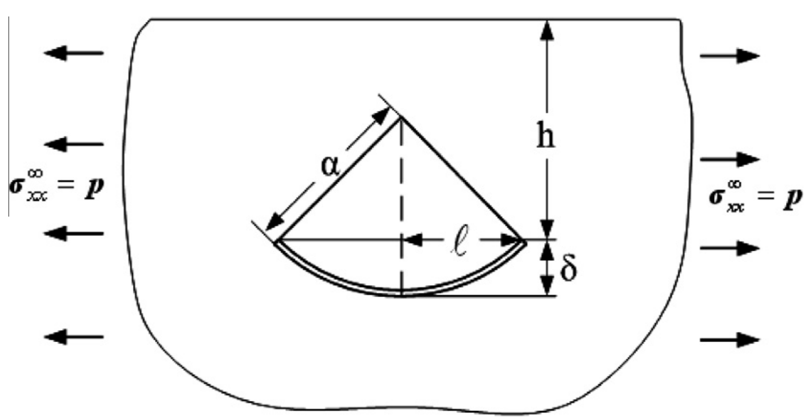

Fig. 8. A curvilinear crack along a part of a circle in the half-plane subjected to far-field horizontal tension.

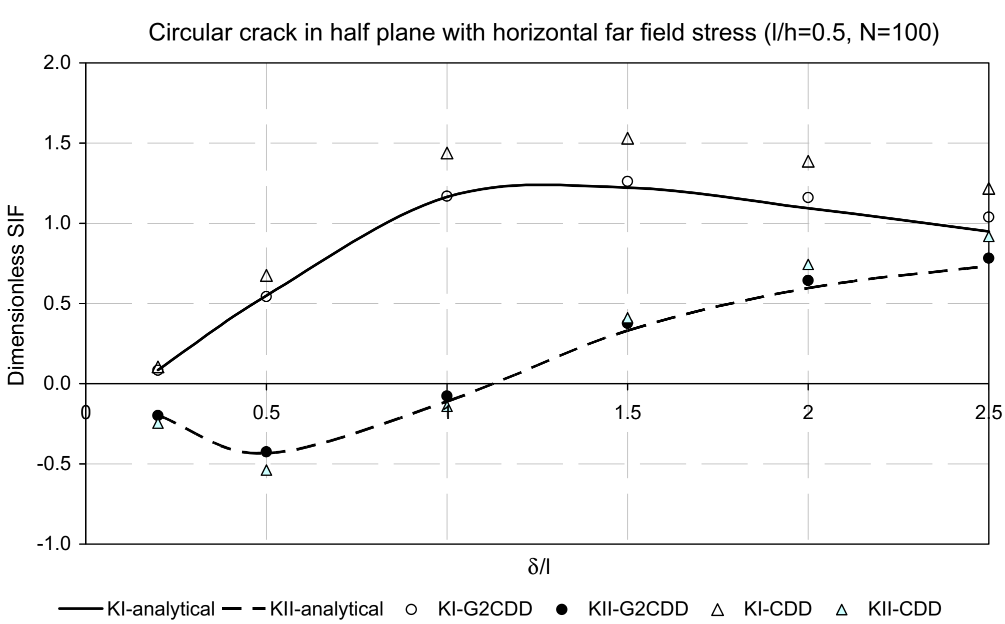

Fig. 9. Variation of modes I and II SIFs with the dimensionless parameter $\delta/\ell$for fixed number of discretization elements ($N = 100$) and relative depth of the crack $\ell/h = 0.5$ as is predicted by the singular integral formulation (referred as "analytical"here) as well as the G2CDD and CDD methods.

worth noticing that the modes I and II SIF's are equal provided that the magnitudes of the far-field tensile and in-plane shear stresses are equal. Therefore, the following diagrams presented in Figs. 6 and 7 are concerned only with the mode I case.

Fig. 6 shows the variation of the dimensionless mode I SIF at the two crack tips A, B as is predicted by the two numerical methods, namely CDD and G2CDD, and by the semi-analytical solution, as the relative crack distance from the free surface increases and for a fixed number of discretization elements of the crack ($N = 50$). On the other hand, the dependence of the SIF on the number of discretization elements for the relative crack depth at hand, is displayed in Fig. 7. From these figures the very nice agreement of the G2CDD method and its superiority compared with the CDD method may be noticed.

3.3. Curvilinear crack close to the boundary

After the first two relative simple problems considered above, we consider the last more complicated problem referred to the first fundamental problem of the theory of elasticity for a half-plane

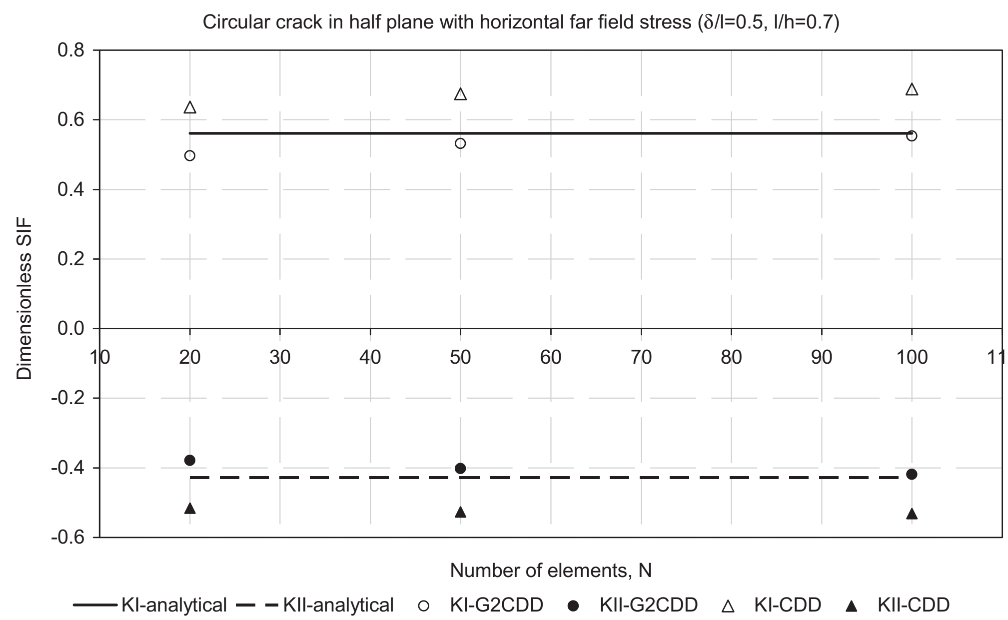

Fig. 10. Variation of mode I and II SIFs with increasing number of discretization elements N for fixed dimensionless parameter $\delta/\ell = 0.5$ and relative depth of the crack $\ell/h = 0.7$ as is predicted by the singular integral formulation (referred as "analytical" here) as well as the G2CDD and CDD methods.

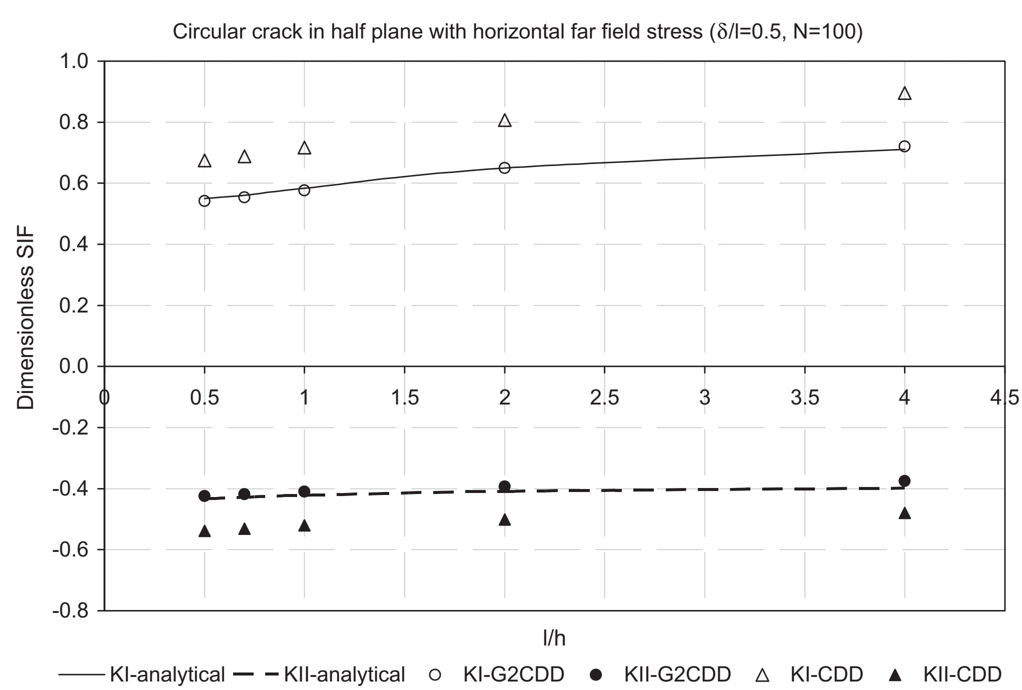

Fig. 11. Variation of modesI and II SIFs with increasing ℓ/h for constant number of discretization elements $N = 100$ and for fixed dimensionless parameter δ/ell;= 0.5 as is predicted by the singular integral formulation (referred as "analytical" here) as wellas the G2CDD and CDD methods.

weakened by curvilinear crack along an arc of a circle, as is displayed in Fig. 8. This problem has been solved by Datsyshin and Marchenko (1984) by virtue of the method of singular integral eqns and Gauss' quadrature formulae. As is shown in the same figure, the half-plane is subjected at infinity with uniform tension $\sigma_{xx}^{\infty} = p > 0$ parallel to the boundary.

In this case Figs. 9–11 present three diagrams in which the predictions for the modes I and II SIF's of the numerical solution of the singular integral formulation (Datsyshin and Marchenko, 1984) are compared with the respective predictions of the G2CDD and CDD methods. From these figures the very close agreement of the G2CDD solution with the singular integral solution for the whole range of the independent variables considered in each case may be observed.

4. Conclusions

The G2CDD element for half-plane problems has been shown to yield results which for the same number of equations, is superior to those achieved using the CDD elements. The test cases have shown that this element is stable and that the numerical results are very close to the correct solutions.

Appendix A. Analytical evaluations of the supplemental stresses for the mode I and II dislocations

The supplemental stress solution for the arbitrarily inclined straight mode I dislocation close to the free surface of the half-space has as follows

$$\begin{aligned}\sigma^{I}_{xx(S)}(x,y) = & -\frac{GD_{\bar{y}}}{2\pi(1-\upsilon)}\Bigg[2\left(\frac{x_r cos\beta - h_r sin\beta}{x_r^2+y_r^2} - \frac{x_\ell cos\beta - h_\ell sin\beta}{x_\ell^2+y_\ell^2}\right)\\ & + 4\left(\frac{x_r cos\beta(h_r y_r - y^2) + h_r y_r sin\beta(y_r - 3y)}{(x_r^2+y_r^2)^2} - \frac{x_\ell cos\beta(h_\ell y_\ell - y^2) + h_\ell y_\ell sin\beta(y_\ell - 3y)}{(x_\ell^2+y_\ell^2)^2}\right)\\ & + 16y\left(\frac{h_r y_r^2(x_r cos\beta + y_r sin\beta)}{(x_r^2+y_r^2)^3} - \frac{h_\ell y_\ell^2(x_\ell cos\beta + y_\ell sin\beta)}{(x_\ell^2+y_\ell^2)^3}\right)\\ & + \ell^2\Bigg\{-2\left(\frac{(x_r(cos(3\beta) - 3cos\beta)(x_r^2 - 3y_r^2) + 4y_r sin^3\beta(y_r - 3x_r^2))}{(x_r^2+y_r^2)^3} - \frac{(x_\ell(cos(3\beta) - 3cos\beta)(x_\ell^2 - 3y_\ell^2) + 4y_\ell sin^3\beta(y_\ell - 3x_\ell^2))}{(x_\ell^2+y_\ell^2)^3}\right)\\ & - 12\left(\frac{(2ysin^3\beta + h_r sin(3\beta))(x_r^4 + y_r^4 - 6x_r^2y_r^2)}{(x_r^2+y_r^2)^4} - \frac{(2ysin^3\beta + h_\ell sin(3\beta))(x_\ell^4 + y_\ell^4 - 6x_\ell^2y_\ell^2)}{(x_\ell^2+y_\ell^2)^4}\right)\\ & - 48\left(\frac{x_r y_r(h_r cos(3\beta) - ycos\beta(cos(2\beta) - 2))(y_r^2 - x_r^2)}{(x_r^2+y_r^2)^4} - \frac{x_\ell y_\ell(h_\ell cos(3\beta) - ycos\beta(cos(2\beta) - 2))(y_\ell^2 - x_\ell^2)}{(x_\ell^2+y_\ell^2)^4}\right)\\ & - 48ycos(3\beta)(\frac{h_r x_r(x_r^4 + 5y_r^4 - 10x_r^2y_r^2)}{(x_r^2+y_r^2)^5} - \frac{h_\ell x_\ell(x_\ell^4 + 5y_\ell^4 - 10x_\ell^2y_\ell^2)}{(x_\ell^2+y_\ell^2)^5})\\ & - 48ysin(3\beta)\left(\frac{h_r y_r(y_r^4 + 5x_r^4 - 10x_r^2y_r^2)}{(x_r^2+y_r^2)^5} - \frac{h_\ell y_\ell(y_\ell^4 + 5x_\ell^4 - 10x_\ell^2y_\ell^2)}{(x_\ell^2+y_\ell^2)^5}\right)\Bigg\}\Bigg]\end{aligned} \tag{A.1a}$$

$$\begin{aligned}\sigma^{I}_{xy(S)}(x,y) = & -\frac{GD_{\bar{y}}y}{2\pi(1-\upsilon)}\Bigg[2\left(\frac{\cos\beta}{x_r^2+y_r^2} - \frac{\cos\beta}{x_\ell^2+y_\ell^2}\right)\\ & + 4\left(\frac{y_r cos\beta(3h_r - y_r) - h_r x_r sin\beta}{(x_r^2+y_r^2)^2} - \frac{y_\ell cos\beta(3h_\ell - y_\ell) - h_\ell x_\ell sin\beta}{(x_\ell^2+y_\ell^2)^2}\right) - 16\left(\frac{h_r y_r^2(y_r cos\beta - x_r sin\beta)}{(x_r^2+y_r^2)^3} - \frac{h_\ell y_\ell^2(y_\ell cos\beta - x_\ell sin\beta)}{(x_r^2+y_r^2)^3}\right)\\ & + 6\ell^2\Bigg\{-\Bigg(\frac{((cos(3\beta) - 3cos(\beta))(x_r^4 + y_r^4 - 6x_r^2y_r^2) - 16x_r y_r sin^3\beta(x_r^2 - y_r^2))}{(x_r^2+y_r^2)^4}\\ & - \frac{((cos(3\beta) - 3cos(\beta))(x_\ell^4 + y_\ell^4 - 6x_\ell^2y_\ell^2) - 16x_\ell y_\ell sin^3\beta(x_\ell^2 - y_\ell^2))}{(x_\ell^2+y_\ell^2)^4}\Bigg) + 8cos(3\beta)\left(\frac{h_r y_r(y_r^4 + 5x_r^4 - 10y_r^2x_r^2)}{(x_r^2+y_r^2)^5} - \frac{h_\ell y_\ell(y_\ell^4 + 5x_\ell^4 - 10x_\ell^2y_\ell^2)}{(x_\ell^2+y_\ell^2)^5}\right)\\ & - 8sin(3\beta)\left(\frac{h_r x_r(x_r^4 + 5y_r^4 - 10x_r^2y_r^2)}{(x_r^2+y_r^2)^5} - \frac{h_\ell x_\ell(x_\ell^4 + 5y_\ell^4 - 10x_\ell^2y_\ell^2)}{(x_\ell^2+y_\ell^2)^5}\right)\Bigg\}\Bigg]\end{aligned} \tag{A.1b}$$

$$\begin{aligned}
\sigma^{I}_{yy(S)}(x,y) = &-\frac{GD_{\bar{y}}}{2\pi(1-\upsilon)}\left[2\left(\frac{x_r cos\beta - h_r sin\beta}{x_r^2+y_r^2}-\frac{x_\ell cos\beta - h_\ell sin\beta}{x_\ell^2+y_\ell^2}\right)\right.\\
&+4\left(\frac{x_r cos\beta(y_r^2+yh_r)+h_r y_r sin\beta(y_r+3y)}{(x_r^2+y_r^2)^2}-\frac{x_\ell cos\beta(y_\ell^2+yh_\ell)+h_\ell y_\ell sin\beta(y_\ell+3y)}{(x_\ell^2+y_\ell^2)^2}\right)\\
&-16y\left(\frac{h_r y_r^2(x_r cos\beta+y_r sin\beta)}{(x_r^2+y_r^2)^3}-\frac{h_\ell y_\ell^2(x_\ell cos\beta+y_\ell sin\beta)}{(x_\ell^2+y_\ell^2)^3}\right)\\
&+\ell^2\left\{-2\left(\frac{(x_r(cos(3\beta)-3cos\beta)(x_r^2-3y_r^2)+4y_r sin^3\beta(y_r-3x_r^2))}{(x_r^2+y_r^2)^3}-\frac{(x_\ell(cos(3\beta)-3cos\beta)(x_\ell^2-3y_\ell^2)+4y_\ell sin^3\beta(y_\ell-3x_\ell^2))}{(x_\ell^2+y_\ell^2)^3}\right)\right.\\
&+12\left(\frac{(2ysin^3\beta-h_r sin(3\beta))(x_r^4+y_r^4-6x_r^2y_r^2)}{(x_r^2+y_r^2)^4}-\frac{(2ysin^3\beta-h_\ell sin(3\beta))(x_\ell^4+y_\ell^4-6x_\ell^2y_\ell^2)}{(x_\ell^2+y_\ell^2)^4}\right)\\
&-48\left(\frac{x_r y_r(h_r cos(3\beta)+ycos\beta(cos(2\beta)-2))(y_r^2-x_r^2)}{(x_r^2+y_r^2)^4}-\frac{x_\ell y_\ell(h_\ell cos(3\beta)+ycos\beta(cos(2\beta)-2))(y_\ell^2-x_\ell^2)}{(x_\ell^2+y_\ell^2)^4}\right)\\
&+48ycos(3\beta)\left(\frac{h_r x_r(x_r^4+5y_r^4-10x_r^2y_r^2)}{(x_r^2+y_r^2)^5}-\frac{h_\ell x_\ell(x_\ell^4+5y_\ell^4-10x_\ell^2y_\ell^2)}{(x_\ell^2+y_\ell^2)^5}\right)\\
&\left.\left.+48ysin(3\beta)\left(\frac{h_r y_r(y_r^4+5x_r^4-10x_r^2y_r^2)}{(x_r^2+y_r^2)^5}-\frac{h_\ell y_\ell(y_\ell^4+5x_\ell^4-10x_\ell^2y_\ell^2)}{(x_\ell^2+y_\ell^2)^5}\right)\right\}\right] \qquad \text{(A.1c)}
\end{aligned}$$

Finally, the supplemental stress solution for the inclined mode II dislocation that interacts with the free surface of a half-space reads as follows

$$\begin{aligned}
\sigma^{II}_{xx(S)}(x,y) = &-\frac{GD_{\bar{x}}}{2\pi(1-\upsilon)}\left[2\left(\frac{h_r cos\beta + x_r sin\beta}{x_r^2+y_r^2}-\frac{h_\ell cos\beta + x_\ell sin\beta}{x_\ell^2+y_\ell^2}\right)\right.\\
&+4\left(\frac{h_r y_r cos\beta(3y-y_r)+y_r sin\beta(h_r y_r-y^2)}{(x_r^2+y_r^2)^2}-\frac{h_\ell y_r cos\beta(3y-y_r)+x_r sin\beta(h_r y_r-y^2)}{(x_\ell^2+y_\ell^2)^2}\right)\\
&-16y\left(\frac{h_r y_r^2(y_r cos\beta-x_r sin\beta)}{(x_r^2+y_r^2)^3}-\frac{h_\ell y_\ell^2(y_\ell cos\beta-x_\ell sin\beta)}{(x_\ell^2+y_\ell^2)^3}\right)\\
&+4\ell^2\left\{-sin\beta\left(\frac{x_r cos(2\beta)(x_r^2-3y_r^2)+y_r sin(2\beta)(3x_r^2-y_r^2)}{(x_r^2+y_r^2)^3}-\frac{x_\ell cos(2\beta)(x_\ell^2-3y_\ell^2)+y_\ell sin(2\beta)(3x_\ell^2-y_\ell^2)}{(x_\ell^2+y_\ell^2)^3}\right)\right.\\
&+3\left(\frac{(h_r cos(3\beta)+ysin\beta sin(2\beta))(x_r^4+y_r^4-6x_r^2y_r^2)}{(x_r^2+y_r^2)^4}-\frac{(h_\ell cos(3\beta)+ysin\beta sin(2\beta))(x_\ell^4+y_\ell^4-6x_\ell^2y_\ell^2)}{(x_\ell^2+y_\ell^2)^4}\right)\\
&+12\left(\frac{x_r y_r(h_r sin(3\beta)-ysin\beta cos(2\beta))(x_r^2-y_r^2)}{(x_r^2+y_r^2)^4}-\frac{x_\ell y_\ell(h_\ell sin(3\beta)-ysin\beta cos(2\beta))(x_\ell^2-y_\ell^2)}{(x_\ell^2+y_\ell^2)^4}\right)\\
&+12ycos(3\beta)\left(\frac{h_r y_r(y_r^4+5x_r^4-10x_r^2y_r^2)}{(x_r^2+y_r^2)^5}-\frac{h_\ell y_\ell(x_\ell^4+5y_\ell^4-10x_\ell^2y_\ell^2)}{(x_\ell^2+y_\ell^2)^5}\right)\\
&\left.\left.-12ysin(3\beta)\left(\frac{h_r x_r(y_r^4+5x_r^4-10x_r^2y_r^2)}{(x_r^2+y_r^2)^5}-\frac{h_\ell x_\ell(y_\ell^4+5x_\ell^4-10x_\ell^2y_\ell^2)}{(x_\ell^2+y_\ell^2)^5}\right)\right\}\right] \qquad \text{(A.2a)}
\end{aligned}$$

$$\begin{aligned}
\sigma^{II}_{xy(S)}(x,y) = &-\frac{GD_{\bar{x}}y}{2\pi(1-\upsilon)}\left[2\left(\frac{\sin\beta}{x_r^2+y_r^2}-\frac{\sin\beta}{x_\ell^2+y_\ell^2}\right)\right.\\
&+4\left(\frac{(h_r x_r cos\beta+y_r sin\beta(3h_r-y_r))}{(x_r^2+y_r^2)^2}-\frac{(h_\ell x_\ell cos\beta+y_\ell sin\beta(3h_\ell-y_\ell))}{(x_\ell^2+y_\ell^2)^2}\right)-16\left(\frac{h_r y_r^2(x_r cos\beta+y_r sin\beta)}{(x_r^2+y_r^2)^3}-\frac{h_\ell y_\ell^2(x_\ell cos\beta+y_\ell sin\beta)}{(x_\ell^2+y_\ell^2)^3}\right)\\
&+12\ell^2\left\{-sin\beta\left(\frac{(cos(2\beta)(x_r^4+y_r^4-6x_r^2y_r^2)+4x_r y_r sin(2\beta)(x_r^2-y_r^2))}{(x_r^2+y_r^2)^4}-\frac{(cos(2\beta)(x_\ell^4+y_\ell^4-6x_\ell^2y_\ell^2)+4x_\ell y_\ell sin(2\beta)(x_\ell^2-y_\ell^2))}{(x_\ell^2+y_\ell^2)^4}\right)\right.\\
&\left.\left.+4cos(3\beta)\left(\frac{h_r x_r(x_r^4+5y_r^4-10x_r^2y_r^2)}{(x_r^2+y_r^2)^5}-\frac{h_\ell x_\ell(x_\ell^4+5y_\ell^4-10x_\ell^2y_\ell^2)}{(x_\ell^2+y_\ell^2)^5}\right)+4sin(3\beta)\left(\frac{h_r y_r(5x_r^4+y_r^4-10x_r^2y_r^2)}{(x_r^2+y_r^2)^5}-\frac{h_\ell y_\ell(5x_\ell^4+y_\ell^4-10x_\ell^2y_\ell^2)}{(x_\ell^2+y_\ell^2)^5}\right)\right\}\right] \qquad \text{(A.2b)}
\end{aligned}$$

$$\begin{aligned}
\sigma^{II}_{yy(S)}(x,y) = & -\frac{GD_{\bar{x}}}{2\pi(1-\nu)}\left[2\left(\frac{h_r cos\beta + x_r sin\beta}{x_r^2+y_r^2} - \frac{h_\ell cos\beta + x_\ell sin\beta}{x_\ell^2+y_\ell^2}\right)\right. \\
& -4\left(\frac{h_r y_r cos\beta(3y+y_r) - x_r sin\beta(yh_r + y_r^2)}{(x_r^2+y_r^2)^2} - \frac{h_\ell y_\ell cos\beta(3y+y_\ell) - x_\ell sin\beta(yh_\ell + y_\ell^2)}{(x_\ell^2+y_\ell^2)^2}\right) \\
& -4y\left(\frac{hr(y_r cos\beta(3x_r^2-y_r^2) - x_r sin\beta(x_r^2-3y_r^2))}{(x_r^2+y_r^2)^3} - \frac{h_\ell(y_\ell \cos\beta(3x_\ell^2-y_\ell^2) - x_\ell \sin\beta(x_\ell^2-3y_\ell^2))}{(x_\ell^2+y_\ell^2)^3}\right) \\
& +4\ell^2\left\{-sin\beta\left(\frac{x_r cos(2\beta)(xr_r^2-3y_r^2) + y_r sin(2\beta)(3x_r^2-y_r^2)}{(x_r^2+y_r^2)^3} - \frac{x_\ell cos(2\beta)(x_\ell^2-3y_\ell^2) + y_\ell sin(2\beta)(3x_\ell^2-y_\ell^2)}{(x_\ell^2+y_\ell^2)^3}\right)\right. \\
& +3\left(\frac{(h_r cos(3\beta) - ysin\beta sin(2\beta))(x_r^4+y_r^4-6x_r^2y_r^2)}{(x_r^2+y_r^2)^4} - \frac{(h_\ell cos(3\beta) - ysin\beta sin(2\beta))(x_\ell^4+y_\ell^4-6x_\ell^2y_\ell^2)}{(x_\ell^2+y_\ell^2)^4}\right) \\
& +12\left(\frac{x_r y_r(h_r sin(3\beta) + ysin\beta cos(2\beta))(x_r^2-y_r^2)}{(x_r^2+y_r^2)^4} - \frac{x_\ell y_\ell(h_\ell sin(3\beta) + ysin\beta cos(2\beta))(x_\ell^2-y_\ell^2)}{(x_\ell^2+y_\ell^2)^4}\right) \\
& -12ycos(3\beta)\left(\frac{h_r y_r(y_r^4+5x_r^4-10x_r^2y_r^2)}{(x_r^2+y_r^2)^5} - \frac{h_\ell y_\ell(y_\ell^4+5x_\ell^4-10x_\ell^2y_\ell^2)}{(x_\ell^2+y_\ell^2)^5}\right) \\
& \left.\left.+12ysin(3\beta)\left(\frac{h_r x_r(x_r^4+5y_r^4-10x_r^2y_r^2)}{(x_r^2+y_r^2)^5} - \frac{h_\ell x_\ell(x_\ell^4+5y_\ell^4-10x_\ell^2y_\ell^2)}{(x_\ell^2+y_\ell^2)^5}\right)\right\}\right]
\end{aligned} \tag{A.2c}$$

wherein

$$\begin{aligned}
x_r &= (x-\cos\beta) \\
x_\ell &= (x+\cos\beta) \\
y_r &= (h-y-\sin\beta) \\
y_\ell &= (h-y+\sin\beta) \\
h_r &= (h-\sin\beta) \\
h_\ell &= (h+\sin\beta)
\end{aligned} \tag{A.3}$$

References

Chen, J.T., Hong, H.-K., 1999. Review of dual boundary element methods with emphasis on hypersingular integrals and divergent series. Appl. Mech. Rev. 52 (1), 17–33.

Crouch, S.L., 1976a. Analysis of stresses and displacements around underground excavations: an application of the Displacement Discontinuity Method, University of Minnesota Geomechanics Report, Minneapolis, Minnesota, November, 1976.

Crouch, S.L., 1976b. Solution of plane elasticity problems by the displacement discontinuity method. Int. J. Numer. Methods Eng. 10, 301–343.

Crouch, S.L., Starfield, A.M., 1990. Boundary Element Methods in Solid Mechanics. Unwin Hyman, Boston.

Datsyshin, A.P., Marchenko, G.P., 1984. Interaction of curvilinear cracks with the boundary of an elastic half-plane. Fiziko-Khimicheskaya Mekhanika Materialov 20 (5), 64–71 [in Russian].

Exadaktylos, G., Xiroudakis, G., 2010a. A G2 constant displacement discontinuity element for analysis of crack problems. Comput. Mech. 45, 245–261.

Exadaktylos, G., Xiroudakis, G., submitted for publication. The G2 constant displacement discontinuity method – Part I: solution of plane crack problems. Int. J. Solids Structures.

Itou, S., 1994. Stress intensity factors around a crack parallel to a free surface of a half-plane. Int. J. Fract. 67, 179–185.

Hirth, J.P., Lothe, J., 1982. Theory of Dislocations. John Wiley and Sons, New York.

Hong, H.-K., Chen, J.T., 1988a. Derivations of integral equations of elasticity. J. Eng. Mech. 114 (6), 1028–1044.

Hong, H.-K., Chen, J.T., 1988b. Generality and special cases of dual integral equations of Elasticity. J. Chin. Soc. Mech. Eng. 9 (1), 1–9.

Tada, H., Paris, P., Irwin, G., 1973. The Stress Analysis of Cracks Handbook. Del Research Corporation, Hellertown, Pennsylvania, pp. 2.1-2.5.